Mol Biotechnol (2017) 59:141–150
DOI 10.1007/s12033-017-0002-2

ORIGINAL PAPER

# Identification and Preparation of a Novel Chemokine Receptor-Binding Domain in the Cytoplasmic Regulator FROUNT

**Akihiro Sonoda[1] · Sosuke Yoshinaga[1] · Kaori Yunoki[1] · Soichiro Ezaki[1] · Kotaro Yano[1] · Mitsuhiro Takeda[1] · Etsuko Toda[2] · Yuya Terashima[2] · Kouji Matsushima[2] · Hiroaki Terasawa[1]**

Published online: 24 March 2017


**Abstract** FROUNT is a cytoplasmic protein that binds to the membrane-proximal C-terminal regions (Pro-Cs) of chemokine receptors, CCR2 and CCR5. The FROUNT–chemokine receptor interactions play a pivotal role in the migration of inflammatory immune cells, indicating the potential of FROUNT as a drug target for inflammatory diseases. To provide the foundation for drug development, structural information of the Pro-C binding region of FROUNT is desired. Here, we defined the novel structural domain (FNT-CB), which mediates the interaction with the chemokine receptors. A recombinant GST-tag-fused FNT-CB protein expression system was constructed. The protein was purified by affinity chromatography and then subjected to in-gel protease digestion of the GST-tag. The released FNT-CB was further purified by anion-exchange and size-exclusion chromatography. Purified FNT-CB adopts a helical structure, as indicated by CD. NMR line-broadening indicated that weak aggregation occurred at sub-millimolar concentrations, but the line-broadening was mitigated by using a deuterated sample in concert with transverse relaxation-optimized spectroscopy. The specific binding of FNT-CB to CCR2 Pro-C was confirmed by the fluorescence-based assay. The improved NMR spectral quality and the retained functional activity of FNT-CB support the feasibility of further structural and functional studies targeted at the anti-inflammatory drug development.

**Keywords** Structural domain · Construct optimization · Chemokine signaling · Cell migration · GPCR · NMR

## Introduction

G-protein-coupled receptors (GPCRs), the largest family of membrane proteins, mediate most cellular responses to hormones and neurotransmitters [1]. Chemokine receptors, which are members of the GPCRs, play an important role in immune cell recruitment to inflammation sites. Among the chemokine receptors, CCR2 and CCR5 are expressed in the membranes of monocytes/macrophages, which play pivotal roles in the inflammatory response [2, 3]. We previously identified the 75-kDa cytoplasmic protein FROUNT, which binds to the cytoplasmic C-terminal regions of CCR2 and CCR5, and activates the chemokine signaling [4, 5]. Furthermore, using a yeast two-hybrid system, we previously clarified that the FROUNT-binding regions of CCR2 and CCR5 are located on the C-terminal membrane-proximal regions [4, 5]. Since FROUNT does not bind to the C-terminal regions of CCR1, CCR3 and CXCR4, FROUNT seems to specifically interact with CCR2 and CCR5 [5].

The potential of FROUNT as a drug development target has been highlighted in various reports, as follows: (1) we previously found that macrophage infiltration was inhibited by FROUNT depletion, in a mouse peritonitis model [4]. (2) Belema-Bedada et al. [6] reported that FROUNT was required for the migration and recruitment of CCR2-expressing bone marrow-derived mesenchymal stem cells to injured heart tissue, using transgenic mice overexpressing

✉ Hiroaki Terasawa
terasawa@structbiol.com

[1] Department of Structural BioImaging, Faculty of Life Sciences, Kumamoto University, 5-1 Oe-honmachi, Chuo-ku, Kumamoto 862-0973, Japan

[2] Department of Molecular Preventive Medicine, Graduate School of Medicine, The University of Tokyo, 7-3-1 Hongo, Bunkyo-ku, Tokyo 113-0033, Japan

CCL2, a ligand of CCR2, in the myocardium. (3) Satoh et al. [7] demonstrated that the mRNA levels of both FROUNT and CCR2 were up-regulated in biopsy tissue samples from patients with heart failure (4) van Golen et al. [8] reported that FROUNT mediates the transendothelial migration of prostate carcinoma cells. These reports confirmed that FROUNT is involved in the migration of various types of cells. However, the mechanism by which FROUNT is regulated in the migration-relevant signal pathway, especially in the initiation of the intracellular signaling cascade, remains elusive. Since FROUNT shares quite low homology with known GPCR regulators, FROUNT may mediate the chemokine signaling in a novel manner. Therefore, clarification of the structure and the function of FROUNT will provide new insights into chemokine signaling and general GPCR regulation.

We previously found that the FROUNT-binding elements of CCR2 and CCR5 lie in their membrane-proximal C-terminal regions (Pro-C), by using the yeast two-hybrid system together with a fluorescence-based assay and a surface plasmon resonance technique [9]. Our recent NMR study revealed that CCR2 Pro-C adopts a typical α-helix when bound to the membrane and a helical conformation when bound to FROUNT [10]. In addition, NMR analyses and mutational studies demonstrated that the binding sites for the membrane and FROUNT were partially overlapped hydrophobic residues [10]. Based on these results, we proposed a model of CCR2 equilibrium: chemokine binding changes the conformational equilibrium of CCR2 toward the active state, and Pro-C switches its binding partner from the membrane to FROUNT [10].

In contrast to the accumulating information about the Pro-C region, our knowledge about FROUNT is still limited. We previously found that the C-terminal fragment from amino acids 500–656 possesses binding affinity for CCR2 Pro-C, indicating that the element responsible for the Pro-C binding lies within this region [4]. To study the Pro-C binding mode by FROUNT, the Pro-C binding structural domain must be identified.

In this study, we defined the Pro-C binding structural domain of FROUNT and established an expression and purification protocol for the recombinant protein of the domain toward structural and functional studies of the interactions between FROUNT and chemokine receptors.

## Materials and Methods

### MS Analysis of the Protease-Resistant Fragments

The protein consisting of amino acids 493–656 of human FROUNT, designated as FNT-CA, which was used in our previous study [9], was digested with α-chymotrypsin (Nacalai Tesque) using 1300 units α-chymotrypsin per gram of protein in PBS buffer (137 mM NaCl, 8.1 mM $Na_2HPO_4$, 2.7 mM KCl and 1.47 mM $KH_2PO_4$, pH 7.4) at 25 °C. After incubations for 0, 3, 15, 60 and 180 min, aliquots of the reaction solutions were obtained, mixed with SDS-PAGE loading buffer and heated for 3 min at 99 °C. The samples were then fractioned on an SDS-PAGE gel under non-reducing conditions. The reaction solution from the incubation for 15 min was desalted with a C18 ZipTip (Merck Millipore), and then analyzed using a MALDI-TOF/TOF ultrafleXtreme spectrometer (Bruker Daltonics).

### Construction of an Expression Vector for FNT-CB

The DNA fragment encoding amino acids 532–656 of human FROUNT was amplified from a template fragment encoding the region of amino acids 493–656 (FNT-CA), by the polymerase chain reaction [PrimeSTAR HS DNA Polymerase (TAKARA)]. The DNA fragment encoding amino acids 532–656 was inserted into the pGEX-4T-3 (GE Healthcare) vector between the *Bam*HI and *Xho*I sites using a Rapid DNA Dephos & Ligation Kit (Roche). The resulting plasmid was named pGEX-4T-3-FNT-C(532–656), and it produces amino acids 532–656 of FROUNT, designated as FNT-CB, fused with a GST-tag at its N-terminus. The linker amino acid sequence between GST and FNT-CB was designed to consist of only the thrombin cleavage site (Leu-Val-Pro-Arg-Gly-Ser), in which the last serine residue also serves as the first amino acid residue of FNT-CB (Ser532).

### Protein Expression

For the production of FNT-CB, *E. coli* BL21 cells were transformed with the pGEX-4T-3-FNT-C(532–656) vector by the calcium chloride method. The resulting colonies were inoculated into 100 mL of LB medium containing ampicillin (50 μg/mL), and the culture was shaken for 12 h at 37 °C. The pre-cultured cells were added into 1 L of LB medium containing ampicillin (100 μg/mL) to achieve an $OD_{600} = 0.1$. The culture was grown at 37 °C with shaking at 150 rpm. When the $OD_{600}$ reached 1.2, isopropyl β-D-1-thiogalactopyranoside (IPTG) was added to a final concentration of 1.0 mM and then the culture was continued with shaking at 130 rpm for 4 h at 32 °C. The culture was centrifuged at 3000×*g* at 4 °C for 10 min, and the resulting cell pellet was collected and frozen at −80 °C. The expression of the recombinant FNT-CA protein was performed using the same procedure as for FNT-CB.

To produce $^{15}N$-labeled proteins, the colonies of the *E. coli* cells were inoculated into 100 mL of LB medium containing 50 μg/mL ampicillin and the culture was incubated at 37 °C with shaking at 180 rpm for 12 h. The culture was centrifuged at 3000×*g* for 10 min at 4 °C, and

the resulting cell pellet was resuspended in 1 L of $H_2O$/M9 medium [5.5 g/L $Na_2HPO_4$ (anhydrous), 2.2 g/L of $KH_2PO_4$ (anhydrous), 0.5 g/L NaCl, 1.0 g/L $^{15}NH_4Cl$ (CIL), 2.0 g/L D-glucose, 1 M $MgSO_4$, 0.1 M $CaCl_2$, 40 mg/L thiamine, 100 mg/L ampicillin and 1.0 g/L CELTONE-N (CIL)] to achieve an $OD_{600} = 0.1$. When the $OD_{600}$ reached 1.2, IPTG was added to induce the recombinant protein expression (final IPTG concentration 1.0 mM). The expression was maintained for 4 h, and then the cells were collected by centrifugation.

For the production of the uniformly $^{2}H/^{15}N$-labeled FNT-CB protein, the pre-culture was initially performed in 100 mL of LB medium for 12 h as described above. The cell pellet was resuspended in 100 mL of the $D_2O$/M9 medium [5.5 g/L $Na_2HPO_4$ (anhydrous), 2.2 g/L of $KH_2PO_4$ (anhydrous), 0.5 g/L NaCl, 1.0 g/L $^{15}NH_4Cl$ (CIL), 2.0 g/L [U-$^{2}H$] D-glucose, 1 M $MgSO_4$, 0.1 M $CaCl_2$, 40 mg/L thiamine, 100 mg/L ampicillin and 1.0 g/L CELTONE-DN (CIL)] to achieve an $OD_{600} = 0.1$. The cells were cultured at 37 °C with shaking (150 rpm) up to an $OD_{600}$ of 3.2, and then the 100 mL culture was added to 900 mL of $D_2O$/M9 medium. The culture was continued for 2.5 h to an $OD_{600}$ of 1.2. The recombinant protein expression was then induced by adding IPTG at the final concentration of 1 mM, and then the culture was maintained for 8 h at 32 °C with shaking at 130 rpm. After the induction period, the cells were collected by centrifugation and stored at −80 °C.

## Protein Purification

The cell pellet was resuspended in 40 mL of buffer A (50 mM Tris–HCl, pH 8.0, 50 mM NaCl, 1 mM DTT and 1 mM EDTA), containing 400 μL of Protease Inhibitor Cocktail (Nacalai Tesque), and lysed by sonication on ice. Triton X-100 was added to the cell lysate at a final concentration of 0.5% to enhance the solubilization of the GST-fused FNT-CB protein. Subsequently, the lysate was centrifuged at 15,000×*g* for 15 min at 4 °C, and the supernatant was filtered through a 0.45 μm filter. The supernatant was absorbed onto a 5-mL bed volume of glutathione Sepharose 4B (GS4B) resin (GE Healthcare), which was pre-equilibrated in buffer A, for 2 h at 4 °C. After the absorption, the resin was loaded into an Econo-Pac chromatography column (10 mL) (Bio-Rad), and the loaded resin was washed initially with 7 mL of buffer A 5 times and then with 7 mL of PBS (137 mM NaCl, 8.1 mM $Na_2HPO_4$, 2.7 mM KCl and 1.47 mM $KH_2PO_4$, pH 7.4). The GS4B resin was then suspended in 7 mL of PBS and transferred to a 15 mL tube. For the in-gel digestion, thrombin protease (ILS) was added to the tube at 5–15 U/mg protein and incubated for 3 h at 23 °C with shaking at 15 rpm. After the thrombin digestion, the released FNT-CB was separated from the resin using an Econo-Pac chromatography column (10 mL) (Bio-Rad). To retrieve the FNT-CB that remained in the resin, 7 mL of buffer A was passed twice through the column. The fractions containing FNT-CB were combined and then supplemented with a 1/100 volume of Protease Inhibitor Cocktail (Nacalai Tesque). To examine whether any undigested GST-fused protein remained, 7 mL of buffer A containing 20 mM reduced glutathione was passed through the resin three times, resulting in the elution of GST and, if present, GST-fused FNT-CB. Aliquots of the solution (13 μL each) were fractionated on an SDS-PAGE gel.

The solution of FNT-CB released from the affinity resin was dialyzed against buffer B (20 mM Tris–HCl, pH 7.5, 1 mM DTT) for 12 h at 4 °C and then loaded onto a Q Sepharose fast flow column (GE Healthcare), pre-equilibrated with buffer B. To ensure the absorption of FNT-CB onto the resin, the resin was kept at 4 °C for 30 min. The impurities were then removed by passing 7 mL of buffer through the resin three times. Subsequently, buffer B containing increasing concentrations of NaCl (i.e., 50, 100, 200 and 300 mM) was passed through the resin. At each NaCl concentration, 7 mL of NaCl-containing buffer B was passed through the resin twice. In the step with 300 mM NaCl, the solution was passed through the resin three times to completely release the absorbent. The fractions eluted at the NaCl concentrations of 50, 100 and 200 mM contained FNT-CB, as determined by an SDS-PAGE analysis. The FNT-CB-containing fractions were pooled and subsequently purified by size-exclusion chromatography [HiLoad 26/60, Superdex 200 prep grade (GE Healthcare)]. The running buffer was 20 mM Tris–HCl, pH 7.5, 50 mM NaCl and 1 mM DTT. The fraction containing FNT-CB was collected and concentrated with a Centriprep YM-3 filter (Millipore). The purity of the prepared FNT-CB was evaluated by an SDS-PAGE analysis. The purification of the recombinant FNT-CA protein was performed using the same procedure as for FNT-CB.

## CD Analysis

The far-UV CD spectra of FNT-CB and FNT-CA were recorded over the range of 200–250 nm at room temperature, with a step size of 0.2 nm, using a JASCO J-820 spectropolarimeter (JASCO). The concentration of the protein was 10–20 μM, and the buffer composition was 50 mM Tris–HCl, pH 7.5, 50 mM NaCl and 1 mM DTT. Spectral deconvolution of CD data was performed using the CDPro software package [11] that consisted of three programs (SELCON3, CDSSTR and CONTINLL) to determine relative quantities of secondary structures.

## NMR Analysis

For NMR experiments, 50 μM of [U-$^{15}N$]-labeled FNT-CA, 100 μM of [U-$^{15}N$]-labeled FNT-CB and 100 μM of

[U-$^{2}$H/$^{15}$N]-labeled FNT-CB were used. The NMR buffer was 20 mM Tris–HCl, pH 7.5, 50 mM NaCl and 1 mM DTT in 95% $H_2O$/5% $D_2O$. The $^{1}$H–$^{15}$N heteronuclear single-quantum correlation (HSQC) spectra were recorded for FNT-CA and FNT-CB. The $^{1}$H–$^{15}$N transverse relaxation-optimized spectroscopy (TROSY)-HSQC spectra [12] were recorded for the [U-$^{15}$N]-labeled FNT-CB and [U-$^{2}$H/$^{15}$N]-labeled FNT-CB. All NMR experiments were performed using an Avance III 600 MHz spectrometer equipped with a cryogenic probe (Bruker BioSpin) at 298 K. The experimental parameters of the HSQC and TROSY-HSQC experiments were identical: the spectral widths were 1500 Hz ($t_1$($^{15}$N)) × 7200 Hz ($t_2$($^{1}$H)), and the data points were 512 ($t_1$) × 1024 ($t_2$). For the processed spectra, the effective data points were 200 ($t_1$) × 1024 ($t_2$). The carrier frequencies of $^{1}$H and $^{15}$N were set to 4.7 and 118 ppm, respectively. The number of scans/FID was 16. The repetition time was 1 s.

### HTRF Assay

The homogeneous time-resolved fluorescence (HTRF) assay [13] was performed using white 384-well low-volume microplates (Corning Coaster). Six different pairs were examined: GST/CCR2 Pro-C, GST/CXCR4 Pro-C, GST-fused FNT-CB/CCR2 Pro-C, GST-fused FNT-CB/CXCR4 Pro-C, GST-fused FNT-CA/CCR2 Pro-C and GST-fused FNT-CA/CXCR4 Pro-C. The reaction solution was prepared by dissolving 25 nM GST, GST-fused FNT-CB or GST-fused FNT-CA, 250 nM biotinylated CCR2 Pro-C peptide or biotinylated CXCR4 Pro-C peptide, 2.6 ng of anti-GST antibody labeled with europium ($Eu^{3+}$) cryptate and 12.5 ng of high-grade XL665-conjugated streptavidin into HTRF buffer (10 mM HEPES–NaOH, pH 7.4, 0.2 M potassium fluoride, 10 mM NaCl, 0.1% Tween 20 and 0.5% BSA). Emissions (Em) at 620 nm and 665 nm wavelengths after excitation at 337 nm were measured at room temperature (25 °C) using an Envision plate reader (PerkinElmer). The fluorescence resonance energy transfer (FRET) intensity was calculated as the $Em_{665nm}/Em_{620nm}$ ratio. Statistical analysis was performed by Tukey's test, and the mean for each group was compared. The significance level was defined as 1%.

## Results and Discussion

### Identification of the Structural Domain in the C-terminal Region of FROUNT

Identification of the structural domains is an initial step in protein structural studies. We began by finding a three-dimensional structure within FNT-CA (residues 493–656), which possesses binding affinity for CCR2 and CCR5 [9]. The recombinant FNT-CA was digested with α-chymotrypsin, and the time course of the digestion was monitored by an SDS-PAGE analysis. With increasing incubation time, a smeared band initially appeared at around 21.5 kDa and then a strong band was detected at a position with an even lower molecular mass. At the 180 min incubation, the smeared band nearly disappeared and the strong band remained (Fig. 1a). The MALDI/TOF MS analysis of the α-chymotrypsin-resistant fragments sampled at the 15 min incubation revealed that the cleavage occurred at the N- or C-terminal peptide bond of Leu531 (Fig. 1b, c). We designated the fragment encompassing the C-terminal 125 amino acids (residues 532–656) as FNT-CB (Fig. 1c, underlined). Note that FNT-CB differs from FNT-CA in that it lacks the N-terminal flanking region (residues 493–531). No protein domains were detected in the FNT-CB region by the SMART domain server [14], and no protein sequences with known structure were detected in this region by the BLASTp sequence server [15]. The identified region was predicted to contain five α-helices (residues 534–548, 553–564, 571–583, 594–608 and 626–650) (Fig. 1c) by an analysis using the PSIPRED secondary structure server [16]. We thus envisaged that the predicted α-helices assemble into a three-dimensional structure and this structural domain may mediate the binding to Pro-C.

### Expression and Purification of the Recombinant FNT-CB Protein

We constructed a vector, pGEX-4T-3-FNT-C(532–656), to produce the recombinant FNT-CB protein. As with the expression vector for FNT-CA [9], the FNT-CB expression vector was designed to produce a fusion protein with a cleavable GST-tag at its N-terminus (Fig. 2). *E. coli* BL21 cells were transformed with the pGEX-4T-3-FNT-C(532–656) vector, and then the cells were cultured in LB medium with ampicillin at 37 °C up to an $OD_{600}$ value of 1.2. The expression of GST-fused FNT-CB was induced by the addition of IPTG at a final concentration of 1 mM. Subsequently, the culture was incubated at 32 °C for 4 h. The $OD_{600}$ value for the IPTG induction and the temperature and duration of the induction were optimized with respect to the protein expression level of the GST-fused FNT-CB in the soluble fraction. At the end of the induction period, the $OD_{600}$ value of the medium reached 2.5. The protein expression was assessed by an SDS-PAGE analysis. In the soluble fraction after the IPTG induction, a strong band appeared around 40 kDa (Fig. 3, lane 4), showing that GST-fused FNT-CB was produced mostly in a soluble form.

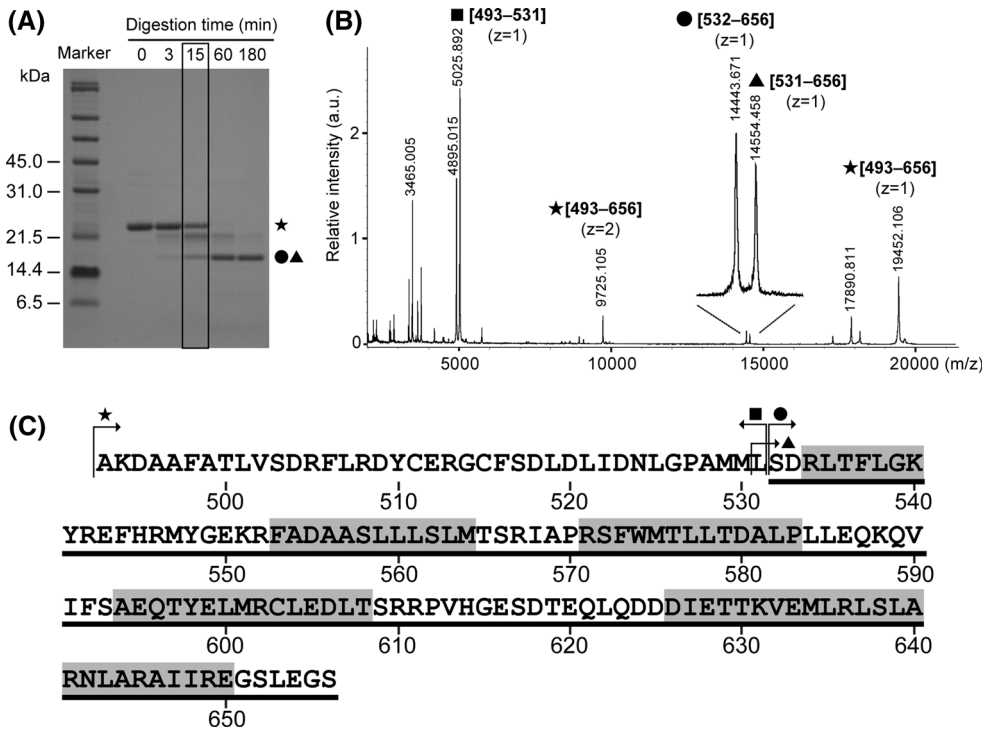


**Fig. 1** **a** Time course of α-chymotrypsin digestion of FNT-CA. The recombinant FNT-CA was incubated in the presence of α-chymotrypsin, and aliquots of the solutions sampled before and after 3, 15, 60 and 180 min were fractionated by SDS-PAGE under non-reducing conditions. **b** MALDI/TOF mass spectrum of the α-chymotrypsin digests of FNT-CA, sampled at the 15 min incubation (*box* in **a**). Each fragment is labeled with the corresponding amino acid region in FNT-CA and the number of charge states. **c** Amino acid sequence of the C-terminal region of FROUNT. The amino acid sequence of FNT-CA (residues 493–656) is presented in the one letter amino acid code. The region corresponding to FNT-CB (residues 532–656) is *underlined*, and the amino acid segments predicted to adopt α-helical structures are tinted in *gray*. The 493–656, 531–656, 532–656 and 493–531 fragments are marked with *a star*, *a triangle*, *a circle* and *a square*, and the bands in **a**, the peaks in **b** and the amino acid regions in **c** are labeled with the corresponding marks

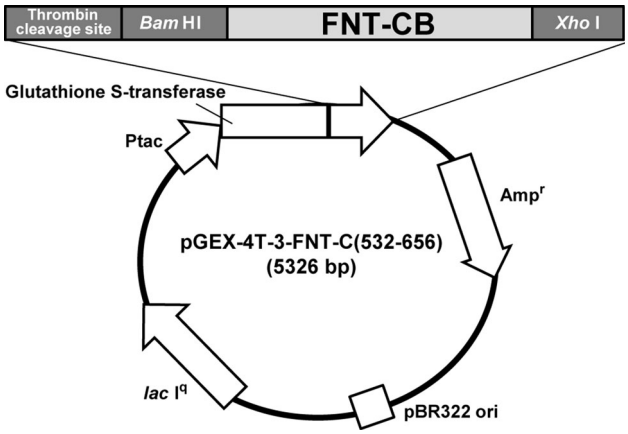


**Fig. 2** Schematic diagram of the FNT-CB expression plasmid. Structure and restriction map of the plasmid pGEX-4T-3-FNT-C(532–656), for the inducible expression of the GST-FNT-CB gene from the tac promoter (Ptac). The vector also contains the ampicillin resistance gene ($Amp^r$), the pBR322 origin of replication (pBR322 ori), and the *lac* $I^q$ gene

For the protein purification, the soluble form of GST-fused FNT-CB (Fig. 4a, lane 2) was initially absorbed onto the glutathione affinity resin, leading to the separation of a

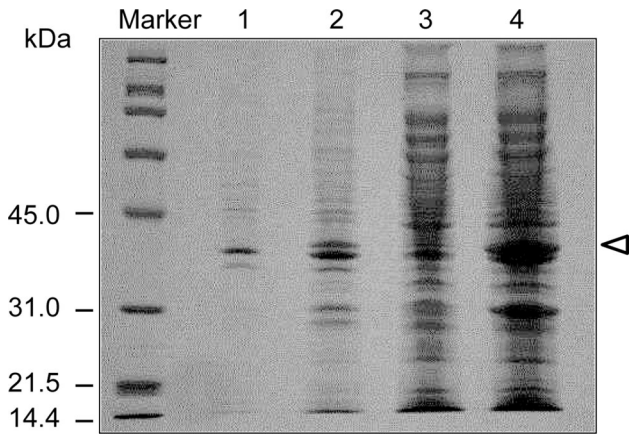


**Fig. 3** Expression profile of the FNT-CB protein from *Escherichia coli* BL21. Insoluble and soluble fractions of a crude bacterial lysate were loaded onto a 15% polyacrylamide gel, and proteins were visualized with Coomassie brilliant blue (CBB). The insoluble fractions before IPTG induction (*lane 1*) and after 4-h induction (*lane 2*) and the soluble fractions before induction (*lane 3*) and after 4-h induction (*lane 4*) were applied. The *white arrowhead* shows the GST-fused FNT-CB protein

large proportion of impurities (Fig. 4a, lanes 3–5) from FNT-CB. Subsequently, the GST-tag was removed by thrombin. We employed an in-gel digestion approach considering the following observations. We previously attempted to digest GST-fused FNT-CA by thrombin after the elution from the glutathione affinity resin. In this case, however, the fusion protein could not be digested efficiently by thrombin, probably due to the aggregation of the fusion proteins. Thus, we alternatively attempted to cleave the fusion protein in the resin-bound state, which substantially improved the digestion efficiency. Likewise, the attempt to apply the in-gel digestion to the GST-fused FNT-CB was successful. After the in-gel digestion, FNT-CB was released from the affinity resin and was detected by SDS-PAGE as a band around 14 kDa (Fig. 4a, lanes 6 and 7). The remaining material bound to the affinity resin was eluted by loading reduced glutathione, and the eluate was subjected to an SDS-PAGE analysis. As a result, the band of GST resulting from the digestion of GST-fused FNT-CB (gray arrow) was detected, while the band of GST-fused FNT-CB, which would appear around 40 kDa, was almost undetectable (Fig. 4a, lanes 9 and 10). Thus, almost all of the GST-fused FNT-CB was successfully cleaved by thrombin with the in-gel digestion method. The removal of the putative aggregation-prone FNT-CA-specific region, in close proximity to the thrombin cleavage site, may suppress the aggregation propensity and facilitate thrombin access to the cleavage site between GST and FNT-CB, in the case of the GST-fused FNT-CB.

The released FNT-CB protein was then purified by anion-exchange chromatography. FNT-CB was absorbed onto the anion-exchange resin, and then the NaCl concentration was increased in a stepwise manner from 0 to 300 mM. As a result, FNT-CB was eluted at NaCl concentrations of 50, 100 and 200 mM (Fig. 4b). The fractions were pooled and subjected to size-exclusion purification. The retention time of FNT-CB was shorter than that expected from its molecular weight as a monomer (14.5 kDa) and was closer to that of the expected dimer (29.0 kDa), as compared with the 28.5-kDa marker protein (Fig. 4c). In contrast, the NMR signals of the eluted FNT-CB protein at a low concentration (micromolar order)

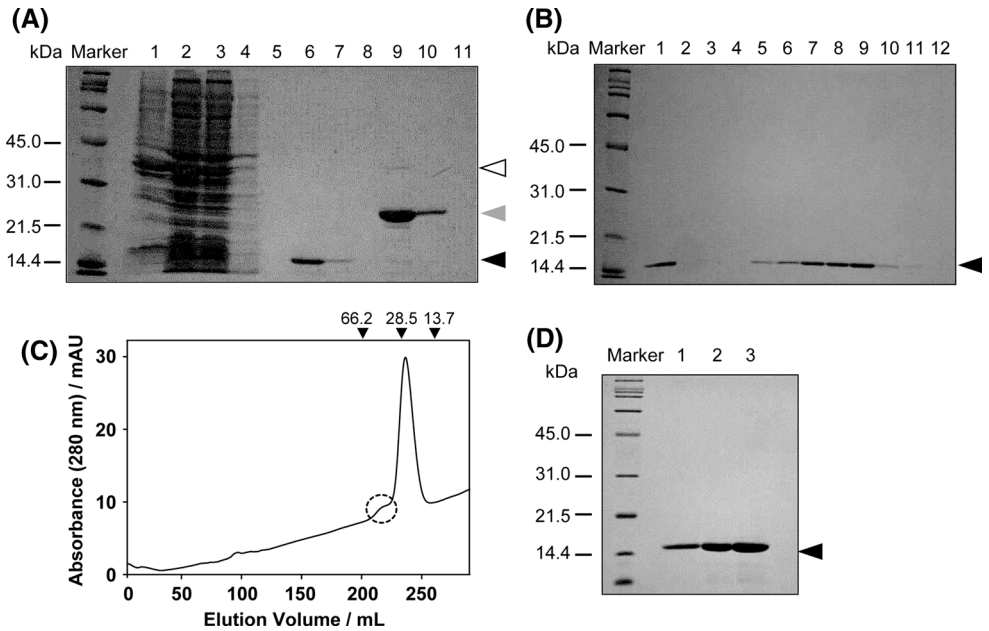


**Fig. 4** Purification of the FNT-CB protein. **a** SDS-PAGE analysis of the glutathione affinity chromatography fractions. *Lanes 1–2*, insoluble and soluble fractions of the crude bacterial lysate after 4-h IPTG induction; *lane 3*, flow through of the soluble fraction from the GS4B column; *lanes 4–5*, wash with buffer A; *lane 6*, flow through of in-gel thrombin cleavage products of the GST-fused FNT-CB protein; *lanes 7–8*, wash with buffer A; *lanes 9–11*, eluates with 20 mM reduced glutathione. The *white*, *black* and *gray arrowheads* show the GST-fused FNT-CB, unfused FNT-CB and GST proteins, respectively. **b** SDS-PAGE analysis of anion-exchange chromatography fractions. *Lane 1*, a mixture of the flow through and wash of the thrombin cleavage products of the GST-fused FNT-CB protein from the GS4B column; *lanes 2–3*, flow through from the Q Sepharose Fast Flow column; *lane 4*, wash with buffer B; *lanes 5–12*, eluates with the 50, 50, 100, 100, 200, 200, 300 and 300 mM NaCl gradient. **c** Size-exclusion chromatogram of FNT-CB separation. The elution volumes of size-exclusion standards are indicated as inverted triangles above the chromatogram: bovine serum albumin (66.2 kDa), bovine carbonic anhydrase (28.5 kDa) and bovine ribonuclease A (13.7 kDa). The main peak has a shoulder corresponding to a putative dimer of FNT-CB (*dashed circle*). **d** SDS-PAGE analysis of the purified FNT-CB protein. Eluted fractions from the size-exclusion chromatography were concentrated to 24 mg/mL. *Lanes 1–3*, aliquots of 2.4, 4.7 and 9.4 μg of the purified FNT-CB protein were subjected to the SDS-PAGE analysis. All fractions in **a**, **b** and **d** were loaded onto a 15% polyacrylamide gel, and the proteins were visualized with CBB

appeared sharp, as expected for a monomer (data not shown). Taken together, we suggest that FNT-CB adopts a non-spherical three-dimensional structure as a monomer with a shorter retention time. The elution peak had a small shoulder with a much shorter retention time (Fig. 4c, dashed circle). Since the intensity of the shoulder peak increased in a manner dependent on the concentration of FNT-CB protein loaded on the column, the shoulder peak presumably corresponds to a dimer of FNT-CB (data not shown).

The fractions of the FNT-CB monomer were combined separately from the putative dimer and then concentrated by centrifugation as the final purification product. The purity of the FNT-CB protein was evaluated to be 99% by an SDS-PAGE analysis (Fig. 4d). As the final product, approximately 9.6 mg of FNT-CB was obtained from 1 L culture in LB medium (Table 1). With a vision toward the NMR study, we also prepared uniformly $^{15}$N-labeled and $^{2}$H/$^{15}$N-labeled FNT-CB by culturing the *E. coli* cells in $H_2O$/M9 and $D_2O$/M9 medium, respectively. The yields of $^{15}$N-labeled and $^{2}$H/$^{15}$N-labeled FNT-CB were 4.3 mg/(1 L culture) and 2.7 mg/(1 L culture), respectively (Table 1). It is noteworthy that the preparation protocol established for FNT-CB can also be used for FNT-CA. However, the purification yield of FNT-CA was 2–3 times lower than that of FNT-CB, possibly due to the lower expression level in the *E. coli* cells and the higher propensity for aggregation.

## Structural Characterization of FNT-CB

The purified FNT-CB protein was analyzed by far-UV CD spectroscopy to examine its secondary structures, for comparison with those of the FNT-CA protein. Negative bands were observed at 222 and 208 nm, indicating that both proteins have helical structures (Fig. 5). The deconvolution of the CD spectra with the CDPro software [11] revealed 49% helical content for FNT-CB and 50% helical content for FNT-CA. The helical content for FNT-CB is qualitatively consistent with the aforementioned secondary structure prediction for the FNT-CB region (Fig. 1). The helical content for FNT-CA implied the presence of helical segments in the N-terminal region, because in FNT-CA, this region is 39 residues larger than that in FNT-CB.

We further characterized FNT-CB by NMR. In general, the dispersion of the amide signals in the $^{1}$H–$^{15}$N HSQC spectrum of a $^{15}$N-labeled protein serves as qualitative evidence of the formation of a three-dimensional structure. For comparison, the recombinant FNT-CA protein was also tested in the HSQC experiment. In the spectrum of FNT-CA, severe crowding of the amide peaks was observed in the region from 7.5 to 8.5 ppm on the $^{1}$H chemical shift scale, and relatively sharper peaks were included among the clustered peaks (Fig. 6a), suggesting the formation of disordered polypeptide segments or transient helices. This situation was improved to some extent in the spectrum of FNT-CB due to the deletion of the FNT-CA-specific region without changing the dispersion pattern of the amide peaks from the structured region (Fig. 6b). The NMR and far-UV CD data indicated that the FNT-CA-specific region may contain transient helical segments, which do not affect the formation of the structural domain in FNT-CB. The line-widths of the amide peaks in FNT-CB were still heterogeneous between different peaks and apparently broader than those expected from its molecular weight as a monomer. When we considered the shoulder peak on the size-exclusion chromatography (Fig. 4c, dashed circle), FNT-CB is partially aggregated at a concentration of 100 μM. As described above, the line-broadening was mitigated by decreasing the sample concentration to the micromolar order. Nevertheless, NMR experiments at such a low concentration would be impractical in terms of sensitivity. We thus attempted to employ the deuteration of FNT-CB [17] in concert with the TROSY method [12], as these approaches are commonly used for NMR studies of high molecular weight proteins. The TROSY method was initially applied for non-deuterated $^{15}$N-labeled FNT-CB. However, it did not appreciably improve the spectral quality (Fig. 6c). By using the deuterated $^{15}$N-labeled FNT-CB protein together with the TROSY method, the line-width of each amide peak became significantly sharpened and almost all of the amide peaks were clearly resolved in the spectrum (Fig. 6d). The quality of the spectrum appeared to be sufficient for proceeding to further multidimensional NMR studies.

**Table 1** Yield of FNT-CB after each purification step from 1 L culture

| | Unlabeled FNT-CB | $^{15}$N-labeled FNT-CB | $^{2}$H/$^{15}$N-labeled FNT-CB |
|---|---|---|---|
| After in-gel digestion on the affinity resin (mg)[a] | 13.4 | 5.9 | 3.7 |
| After anion-exchange chromatography (mg)[a] | 12.0 | 5.3 | 3.3 |
| After size-exclusion chromatography (mg)[a] | 9.6 | 4.3 | 2.7 |
| Purity (%) | 99 | 99 | 99 |

[a] The yield of the FNT-CB protein was estimated by comparing the band intensity with 0.5 μg of lysozyme on a CBB-stained SDS-PAGE gel

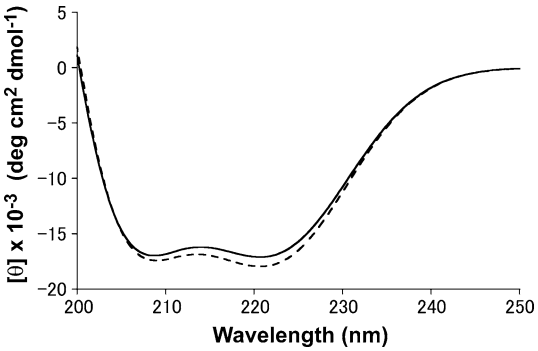


**Fig. 5** CD spectra of the FNT-CA and FNT-CB proteins. The far-UV CD spectra were acquired at room temperature. The *solid* and *dashed lines* show the spectra of FNT-CB and FNT-CA, respectively. The protein sample was prepared in 50 mM Tris–HCl, pH 7.5, 50 mM NaCl and 1 mM DTT

### Chemokine Receptor-Binding Activity of FNT-CB

We examined whether FNT-CB actually retains the binding activity to CCR2 Pro-C. Referring to the previous binding assay [9], the binding of FNT-CB to CCR2 Pro-C and, as a negative control, CXCR4 Pro-C, and the binding of FNT-CA to the Pro-Cs were examined by the HTRF method [13]. In this experiment, GST-fused FNT-CB or FNT-CA was detected by an anti-GST antibody conjugated with $Eu^{3+}$ cryptate (donor fluorophore), and the biotin-conjugated Pro-C peptide was detected by streptavidin conjugated to XL665 (acceptor fluorophore). If either FNT-CB or FNT-CA interacts with the Pro-Cs, then the coupled donor and acceptor fluorophores will approach each other. Thus, the fluorescent emission at 620 nm from the donor fluorophore would be efficiently transferred to XL665, resulting in a fluorescent emission at 665 nm. The FRET intensity observed for the pairs of GST-fused FNT-CB/CCR2 Pro-C and GST-fused FNT-CA/CCR2 Pro-C was significantly higher than that detected in the reference experiment (i.e., the pair of GST and CCR2 Pro-C) (Fig. 7). In contrast, in the experiment using CXCR4 Pro-C, the increase of the FRET signal relative to the reference experiment was marginal. These results were qualitatively consistent with the findings that FROUNT binds to CCR2, but not to CXCR4 [4, 5, 9, 10]. Thus, we concluded that the identified structural domain possesses significant binding affinity to CCR2 Pro-C. The FRET intensity detected for

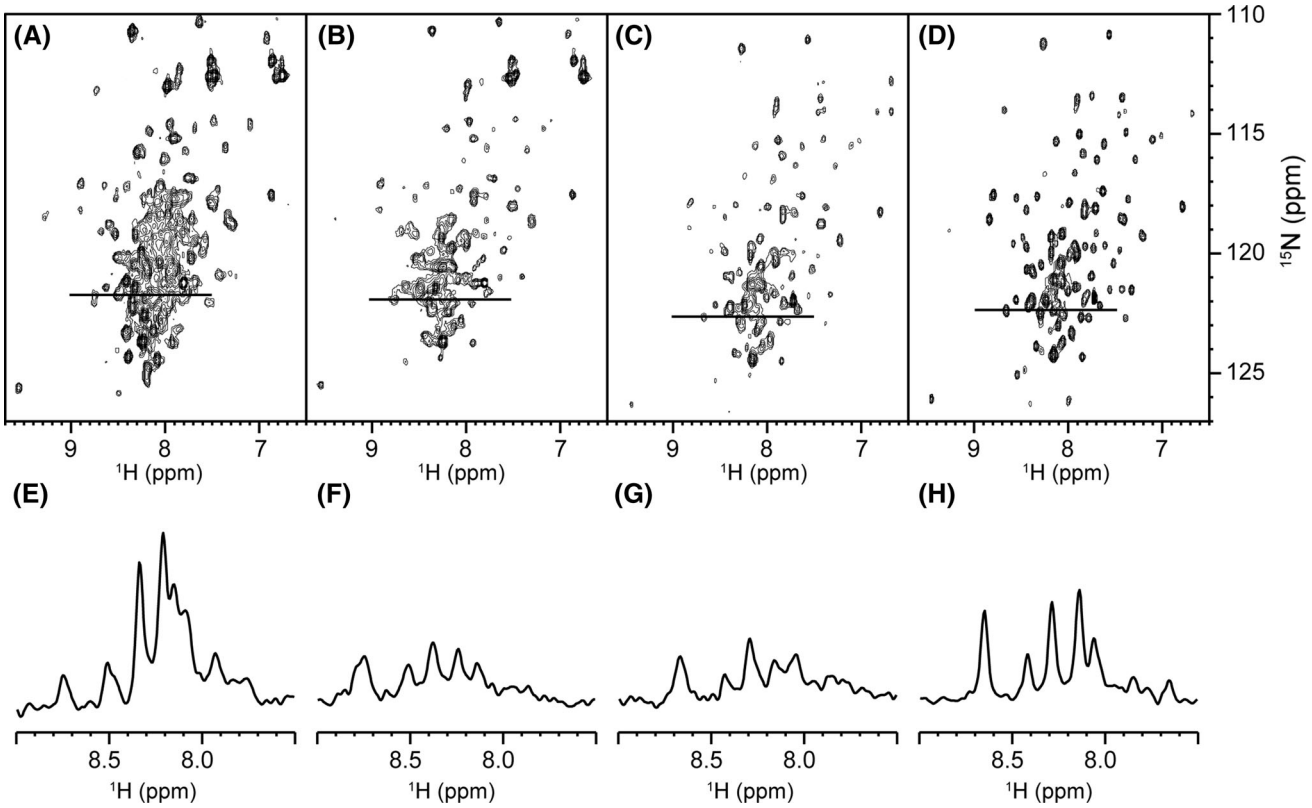


**Fig. 6** $^{1}H$–$^{15}N$ HSQC spectra recorded on $^{15}N$-labeled FNT-CA (**a**) and FNT-CB (**b**) and the $^{1}H$–$^{15}N$ TROSY-HSQC spectra of $^{15}N$-labeled FNT-CB (**c**) and $^{2}H/^{15}N$-labeled FNT-CB (**d**). Slices along the *horizontal lines* in **a**, **b**, **c** and **d** are displayed in **e**, **f**, **g** and **h**, respectively. The spectra were acquired at 298 K on a 600 MHz spectrometer with a cryogenic probe. The concentration of $^{15}N$-labeled FNT-CA was 50 μM, and those of $^{15}N$-labeled and $^{2}H/^{15}N$-labeled FNT-CB were both 100 μM. The samples were dissolved in buffer containing 20 mM Tris–HCl, pH 7.5, 50 mM NaCl and 1 mM DTT, prepared in 95% $H_2O$ and 5% $D_2O$

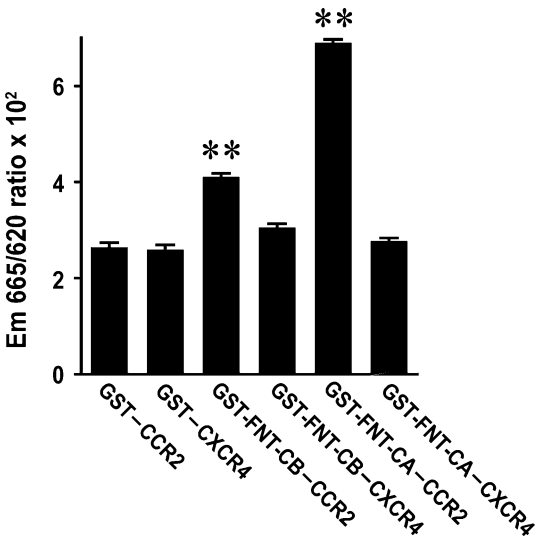


**Fig. 7** CCR2 Pro-C binding activity of FNT-CB. The ability of the FNT-CB protein to bind to the CCR2 Pro-C peptide was examined by an HTRF assay using an indirect 'cassette format,' in which the interaction between GST-fused FNT-CB and the biotinylated CCR2 Pro-C peptide was detected by an anti-tag donor/acceptor pair, namely cryptate-labeled anti-GST antibodies and a streptavidin-XL665 conjugate, respectively. Results are mean ± S.D. $^{**}P < 0.01$. GST or GST-fused FNT-CA protein and the biotinylated CXCR4 Pro-C peptide were used as controls

the FNT-CA/CCR2 Pro-C pair was approximately 1.7 times higher than that for the FNT-CB/CCR2 Pro-C pair (Fig. 7). The intensity difference might be explained by the clustering effect of FNT-CA. As described above, FNT-CA is more prone to aggregation than FNT-CB, and thus a CCR2 Pro-C molecule that has just dissociated from one FNT-CA soon encounters another FNT-CA in close proximity, which apparently increases the population of the CCR2-bound form, as compared with the FNT-CB/CCR2 Pro-C pair.

## Conclusions

In the present study, we identified the structural domain in FROUNT responsible for binding to the chemokine receptor and established the expression and purification protocol for the recombinant protein using an *E. coli* expression system. The availability of a high-quality HSQC spectrum is a milestone in the NMR study. We have embarked on the structural analysis of the FNT-CB–CCR2 Pro-C interaction, including NMR signal assignment and ligand titration experiments. Finally, it is our sincere hope that this study will contribute to develop therapeutic drugs for various inflammatory diseases, such as heart diseases and cancers.

**Acknowledgements** We are grateful to Dr. Shogo Misumi for the MALDI/TOF MS measurements. This work was supported in part by the Targeted Proteins Research Program (TPRP) from the Ministry of Education, Culture, Sports, Science and Technology of Japan (MEXT) (to S.Y., E.T., Y.T., K.M. and H.T.), by Practical Research for Innovative Cancer Control from the Japan Agency for Medical Research and Development (AMED) (to S.Y., E.T., Y.T., K.M. and H.T.), by Project for Development of Innovative Research on Cancer Therapeutics (P-DIRECT) from AMED (to S.Y., M.T., Y.T., K.M. and H.T.), by a Grant-in-Aid for Young Scientists (B) (JP19790064) from MEXT (to S.Y.), by the KUMAYAKU Alumni Research Fund (to S.Y.), by a Sasakawa Scientific Research Grant from the Japan Science Society (to K.Y.), by the Global COE Program-Cell Fate Regulation Research and Education Unit from MEXT (to K.Y.), by the Adaptable and Seamless Technology Transfer Program through target-driven R & D (A-STEP), Japan Science and Technology Agency (JST) (to H.T.) and by the Cooperative Research Project Program of the Medical Institute of Bioregulation, Kyushu University (to H.T.).

## References

1. Rosenbaum, D. M., Rasmussen, S. G. F., & Kobilka, B. K. (2009). The structure and function of G-protein-coupled receptors. *Nature, 459*(7245), 356–363. doi:10.1038/nature08144.
2. Charo, I. F., Myers, S. J., Herman, A., Franci, C., Connolly, A. J., & Coughlin, S. R. (1994). Molecular cloning and functional expression of two monocyte chemoattractant protein 1 receptors reveals alternative splicing of the carboxyl-terminal tails. *Proceedings of the National Academy of Sciences of the United States of America, 91*(7), 2752–2756.
3. Kraft, K., Olbrich, H., Majoul, I., Mack, M., Proudfoot, A., & Oppermann, M. (2001). Characterization of sequence determinants within the carboxyl-terminal domain of chemokine receptor CCR5 that regulate signaling and receptor internalization. *The Journal of biological chemistry, 276*(37), 34408–34418. doi:10.1074/jbc.M102782200.
4. Terashima, Y., Onai, N., Murai, M., Enomoto, M., Poonpiriya, V., Hamada, T., et al. (2005). Pivotal function for cytoplasmic protein FROUNT in CCR2-mediated monocyte chemotaxis. *Nature Immunology, 6*(8), 827–835. doi:10.1038/ni1222.
5. Toda, E., Terashima, Y., Sato, T., Hirose, K., Kanegasaki, S., & Matsushima, K. (2009). FROUNT is a common regulator of CCR2 and CCR5 signaling to control directional migration. *Journal of Immunology, 183*(10), 6387–6394. doi:10.4049/jimmunol.0803469.
6. Belema-Bedada, F., Uchida, S., Martire, A., Kostin, S., & Braun, T. (2008). Efficient homing of multipotent adult mesenchymal stem cells depends on FROUNT-mediated clustering of CCR2. *Cell Stem Cell, 2*(6), 566–575. doi:10.1016/j.stem.2008.03.003.
7. Satoh, M., Akatsu, T., Ishkawa, Y., Minami, Y., & Nakamura, M. (2007). A novel activator of C–C chemokine, FROUNT, is expressed with C–C chemokine receptor 2 and its ligand in failing human heart. *Journal of Cardiac Failure, 13*(2), 114–119. doi:10.1016/j.cardfail.2006.11.003.
8. van Golen, K. L., Ying, C., Sequeira, L., Dubyk, C. W., Reisenberger, T., Chinnaiyan, A. M., et al. (2008). CCL2 induces prostate cancer transendothelial cell migration via activation of the small GTPase Rac. *Journal of Cell Biochemistry, 104*(5), 1587–1597. doi:10.1002/jcb.21652.
9. Toda, E., Terashima, Y., Esaki, K., Yoshinaga, S., Sugihara, M., Kofuku, Y., et al. (2014). Identification of a binding element for the cytoplasmic regulator FROUNT in the membrane-proximal carboxy-terminal region of chemokine receptors CCR2 and

CCR5. *Biochemical Journal, 457*(2), 313–322. doi:10.1042/BJ20130827.
10. Esaki, K., Yoshinaga, S., Tsuji, T., Toda, E., Terashima, Y., Saitoh, T., et al. (2014). Structural basis for the binding of the membrane-proximal C-terminal region of chemokine receptor CCR2 with the cytosolic regulator FROUNT. *The FEBS Journal, 281*(24), 5552–5566. doi:10.1111/febs.13096.
11. Sreerama, N., & Woody, R. W. (2000). Estimation of protein secondary structure from circular dichroism spectra: comparison of CONTIN, SELCON, and CDSSTR methods with an expanded reference set. *Analytical Biochemistry, 287*(2), 252–260. doi:10.1006/abio.2000.4880.
12. Pervushin, K., Riek, R., Wider, G., & Wüthrich, K. (1997). Attenuated T2 relaxation by mutual cancellation of dipole-dipole coupling and chemical shift anisotropy indicates an avenue to NMR structures of very large biological macromolecules in solution. *Proceedings of the National Academy of Sciences of the United States of America, 94*(23), 12366–12371.
13. Mathis, G. (1995). Probing molecular interactions with homogeneous techniques based on rare earth cryptates and fluorescence energy transfer. *Clinical Chemistry, 41*(9), 1391–1397.
14. Letunic, I., Doerks, T., & Bork, P. (2015). SMART: recent updates, new developments and status in 2015. *Nucleic Acids Research, 43,* D257–D260. doi:10.1093/nar/gku949.
15. Boratyn, G. M., Camacho, C., Cooper, P. S., Coulouris, G., Fong, A., Ma, N., et al. (2013). BLAST: a more efficient report with usability improvements. *Nucleic Acids Research, 41,* W29–W33. doi:10.1093/nar/gkt282.
16. Buchan, D. W. A., Minneci, F., Nugent, T. C. O., Bryson, K., & Jones, D. T. (2013). Scalable web services for the PSIPRED Protein Analysis Workbench. *Nucleic Acids Research, 41,* W349–W357. doi:10.1093/nar/gkt381.
17. Gardner, K. H., & Kay, L. E. (1998). The use of $^{2}H$, $^{13}C$, $^{15}N$ multidimensional NMR to study the structure and dynamics of proteins. *Annual Review of Biophysics and Biomolecular Structure, 27,* 357–406. doi:10.1146/annurev.biophys.27.1.357.